Raman-Kerr Combs in High-Q Chalcogenide Microresonators Coupled to Silicon Waveguides

Philippe Jean, Alexandre Douaud, Sophie LaRochelle, Younès Messaddeq and Wei Shi

Centre d'Optique, Photonique et Laser (COPL), Université Laval, Québec, QC, Canada

wei.shi@gel.ulaval.ca

Abstract: We report the observation of Kerr frequency combs and Raman lasing in a high-Q (Q>1.5e6) $As_{20}S_{80}$ microresonator monolithically integrated with silicon-on-insulator waveguides.

Chalcogenide glasses (ChG) are attractive candidates for integrated nonlinear photonics due to their strong third-order nonlinear response, broad spectral transparency and overall flexibility [1]. Yet, interest in these glasses for the near-infrared (NIR) is mitigated by currently achievable propagation losses in compact structures and the practical absence of a component library. A solution to the latter is to co-integrate chalcogenide structures on the silicon-on-insulator (SOI) platform to combine the advantages of chalcogenide with the vast silicon passive and active component library [2]. Yet, achieving high-Q ($Q > 1 \times 10^6$) in ChG microresonators (MRs) is usually limited to weakly confined structures based on shallow etch or indirect etching that require mm-scale bend radius to prevent radiation losses [3]. In this work, we report the observation of Raman lasing and optical parametric oscillation in a high quality factor ($Q > 1.5 \times 10^6$) and compact ($R = 100\,\mu$m) ChG MR monolithically integrated with silicon-on-insulator waveguides.

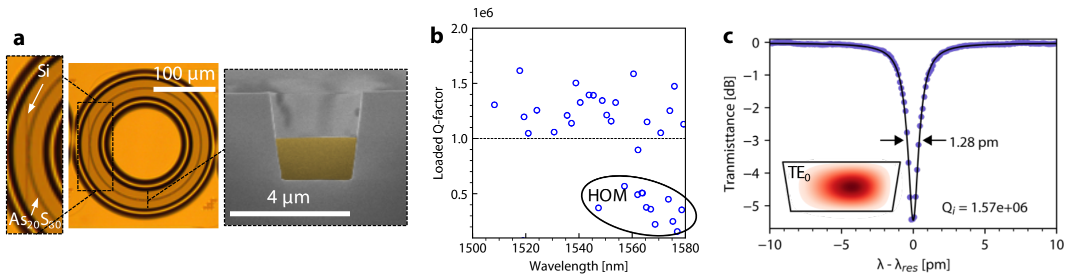

Fig. 1. Chalcogenide-silicon microresonator. (a) Micrograph of a MR with (right inset) a false-color SEM image of the $As_{20}S_{80}$ waveguide cross-section and (left inset) a close-up view of the coupling region. (b) Measured loaded Q-factor of an undercoupled MR with multimode operation past 1540 nm (HOM = higher order modes). (c) Measured (dots) and fitted (line) single resonance around 1536 nm with $Q_i = 1.57 \times 10^6$ and (inset) the simulated fundamental quasi-TE mode electric field intensity profile supported in the curved waveguide.

The chips were fabricated using standard in-foundry 220 nm SOI processing and in-house post-processing for the ChG MRs. The fabrication process is presented in more details in ref. [4]. The post-processing is based on micro-trench filling and thermal annealing well over the glass transition temperature (T_g), which serves to break the film metastability, leading to a spontaneous reorganization into equilibrium shapes (i.e. dewetting). The resulting MRs are shown in Fig.1(a), where the right inset shows a false-color scanning electron microscope (SEM) image of a focused ion beam (FIB) cut of the chip, revealing a nicely shaped waveguide formed by dewetting and the left inset is a zoomed view of the coupling region between the tapered silicon bus waveguide and the ChG MR. The low power response of the hybrid MRs were measured using a laser-scan technique in the C-band on a 0.1 pm grid with fiber-to-chip coupling using lensed fibers and silicon waveguide inverse tapers. The results are summarized in Fig.1 (b) and (c) for the quasi-TE modes. Fig.1(b) presents the loaded Q-factor (Q_L) of the MR measured at resonances over a 80 nm span and confirms the high-Q behavior of the MR. At longer wavelengths, the mode from the silicon bus waveguide resulted in the excitation of higher order transverse modes inside the MR, these modes had significantly lower Qs, as shown by the encircled data in Fig.1(b). Fig.1(c) shows a single undercoupled resonance near 1536 nm along with a Lorentzian fit that indicates a narrow linewidth at mid-height of 1.28 pm, corresponding to an unloaded Q-factor of 1.57×10^6, one of the highest measured in this work.

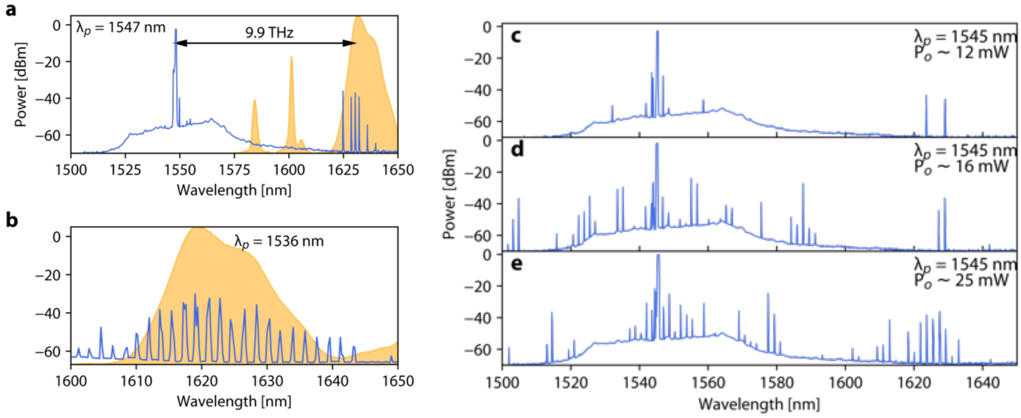

Fig. 2. Experimental observations of Raman lasing and Kerr combs in a hybrid MR. (a) Few lines Raman comb when pumping near 1547 nm. (b) Raman comb when pumping a high-Q resonance near 1536 nm. The shaded curves in (a) and (b) show the Raman response spectrum of bulk $As_{20}S_{80}$. (c),(d),(e) Co-existence of Raman comb and Kerr combs components when pumping near 1545 nm at on-chip pump power of 12 mW, 16 mW and 25 mW, respectively.

Next, the nonlinear response of the MR was investigated by scanning high-Q resonances with an amplified tunable laser. The results for different resonances and powers are summarized in Fig.2. The pump laser and the cavity could not be locked together passively as the glass photosensitivity in the NIR resulted in permanent red-shift even for moderate power and the thermal effects caused unstable operation, preventing in-depth analysis of lasing threshold, noise performance or even high resolution measurement. In order to extract the laser spectrum, the resonance under study was continuously scanned with the tunable laser while the ouput was accumulated on an optical spectrum analyzer. A few examples of observed Raman combs are presented in Fig.2 (a) and (b) for pump power and wavelength combinations of 16 mW at 1547 nm and 50 mW at 1536 nm, respectively. The Raman gain spectra of $As_{20}S_{80}$ (shown as orange shading in Fig.2 (a) and (b)) was measured by Raman spectroscopy for comparison with the achieved Raman combs and shows good agreement with the strongest gain peak located at a 9.9 THz frequency shift. Co-existence of Raman lasing and Kerr components was also observed at different pump power, as shown in 2 (c) through (d). Increasing the pump power resulted in additional frequency components attributed to cascading of the Kerr combs as well as four-wave mixing with the Raman comb. The uneven shape and distribution of the Kerr combs is attributed to the low coupling ideality of the hybrid MR, resulting in strong coupling variations and excitation of low-Q higher order modes.

This work is the first demonstration of Raman lasing and optical parametric oscillation in a hybrid ChG-Si platform and represents an important milestone towards monolithic efficient and compact chalcogenide nonlinear photonics components compatible with SOI fabrication. Improving on this proof-of-concept will require addressing the photosensitivity and thermal instabilities of the MR to achieve stable laser operation.

Acknowledgements: We acknowledge the support of the National Sciences and Engineering Research Council through strategic project grant (STPGP 494358-16).

References

1. B. J. Eggleton, B. Luther-Davies, and K. Richardson, “Chalcogenide photonics,” Nat. Photonics **5**, 141–148 (2011).
2. Y. Liu, A. Choudhary, G. Ren, K. Vu, B. Morrison, A. Casas-Bedoya, T. G. Nguyen, D.-Y. Choi, P. Ma, A. Mitchell, S. J. Madden, D. Marpaung, and B. J. Eggleton, “Integration of brillouin and passive circuits for enhanced radio-frequency photonic filtering,” APL Photonics **4**, 106103 (2019).
3. D.-G. Kim, S. Han, J. Hwang, I. H. Do, D. Jeong, J.-H. Lim, Y.-H. Lee, M. Choi, Y.-H. Lee, D.-Y. Choi, and H. Lee, “Universal light-guiding geometry for on-chip resonators having extremely high q-factor,” Nat. Commun. **11**, 5933 (2020).
4. P. Jean, A. Douaud, V. Michaud-Belleau, S. H. Messaddeq, J. Genest, S. LaRochelle, Y. Messaddeq, and W. Shi, “Etchless chalcogenide microresonators monolithically coupled to silicon photonic waveguides,” Opt. Lett. **45**, 2830–2833 (2020).